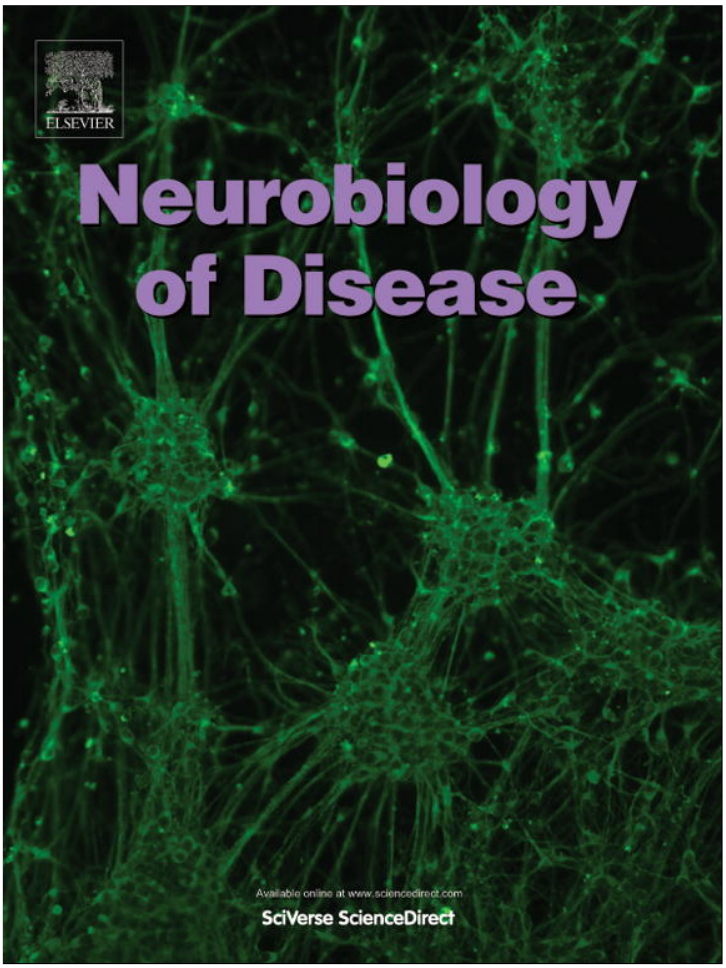

(This is a sample cover image for this issue. The actual cover is not yet available at this time.)

Neurobiology of Disease 48 (2012) 454–463

Contents lists available at SciVerse ScienceDirect

Neurobiology of Disease

journal homepage: www.elsevier.com/locate/ynbdi

Long-term genetic fate mapping of adult generated neurons in a mouse temporal lobe epilepsy model

Mehrnoosh Jafari [a,d], Jonna Soerensen [a], Renée Marie Bogdanović [a,d], Leda Dimou [b,c], Magdalena Götz [b,c], Heidrun Potschka [a,*]

[a] Institute of Pharmacology, Toxicology, and Pharmacy, Ludwig–Maximilians-University Munich, Germany
[b] Institute of Stem Cell Research, Helmholtz Zentrum Muenchen, Neuherberg, Munich, Germany
[c] Physiological Genomics, Ludwig–Maximilians-University, Munich, Germany
[d] Graduate School of Systemic Neurosciences, Ludwig–Maximilians-University, Munich, Germany

ARTICLE INFO

Article history:
Received 13 December 2011
Revised 15 June 2012
Accepted 22 June 2012
Available online 30 June 2012

Keywords:
GLAST
CreERT2
eGFP
Adult neurogenesis
Neuron integration

ABSTRACT

In the epileptic brain, seizures can increase hippocampal neurogenesis, while opposingly seizure-associated brain pathology has been shown to detrimentally affect neurogenesis. The long-term impact of recurrent seizures on the number of new neurons as well as their relative contribution to the granule cell layer remains an open question. Therefore we analyzed neuron addition based on genetic fate mapping in a chronic model of epilepsy comparing non-kindled animals and kindled animals having at least one generalized seizure with and without further seizures.

The number of all new granule cells added to the dentate gyrus following the onset of kindling was significantly increased (7.0–8.9 fold) in kindled groups. The hyperexcitable kindled state and a prior seizure history proved to be sufficient to cause a pronounced long-term net effect on neuron addition. An ongoing continuous occurrence of seizures did not further increase the number of new granule cells in the long-term. In contrast, a correlation was found between the cumulative duration of seizures and neuron addition following a kindled state.

In addition, the overall number of seizures influenced the relative portion of new cells among all granule cells. Non-kindled animals showed 1.6% of new granule cells among all granular cells by the end of the experiment. This portion reached 5.7% in the animals which experienced either 10 or 22 seizures. A percentage of 8.4% new cells were determined in the group receiving 46 seizures which is a significant increase in comparison to the control group.

In conclusion, permanent genetic fate mapping analysis demonstrated that recurrent seizures result in a lasting change in the makeup of the granule cell layer with alterations in the relative contribution of newborn neurons to the granule cell network. Interestingly, the formation of a hyperexcitable kindled network even without recent seizure activity can result in pronounced long-term alterations in the absolute number of new granule cells. However, seizure density also seems to play a critical role with more frequent seizures resulting in increased fractions of new neurons.

Seizures can increase neurogenesis in the subgranular zone of the dentate gyrus, one of the major neurogenic zones of the adult brain (Danzer, 2012; Kokaia, 2011; Parent and Murphy, 2008; Scharfman and McCloskey, 2009). Studies in chronic rodent models of epilepsy including the kindling model and post-status epilepticus models repeatedly demonstrate a considerable expansion of newborn granule cells when seizure activity is induced in naïve animals (Parent et al., 1998, 1999; Scott et al., 1998). In post-status epilepticus models, increased hippocampal neurogenesis characterizes the latent phase; however, in several studies with chemically-induced status epilepticus animals exhibited a reduced neurogenesis in the chronic phase with spontaneous recurrent seizures (Hattiangady and Shetty, 2010; Hattiangady et al., 2004). Evidence exist that hippocampal pathology including cell loss and gliosis can affect the neurogenic niche resulting in decreased survival or neuronal differentiation of progenitor cells (Hattiangady and Shetty, 2010). On the other hand, Cha et al. (2004) reported that spontaneous recurrent seizures in the chronic phase can further enhance dentate gyrus neurogenesis.

Respective findings raise the question to what extent the generation of a hyperexcitable network and subsequent recurrent chronic seizures affect the long-term overall balance of hippocampal neurogenesis. Previous studies have been based on administration of DNA

* Corresponding author at: Institute of Pharmacology, Toxicology, and Pharmacy, Ludwig–Maximilians-University, Koeninginstr, 16, D-80539 Munich, Germany. Fax: +49 89 218016556.
E-mail address: potschka@pharmtox.vetmed.uni-muenchen.de (H. Potschka).
Available online on ScienceDirect (www.sciencedirect.com).

0969-9961/$ – see front matter © 2012 Elsevier Inc. All rights reserved.
doi:10.1016/j.nbd.2012.06.014

base analogs or infection with retroviral vectors (Parent et al., 2002; Taupin, 2007a,b). Conclusions from these investigations are limited by the fact that only a small cohort of adult-generated cells is labeled. Moreover, BrdU labeling gives information about only a limited time window. It is well known that the indirect extrapolation of respective data can lead to diverse predictions of overall neuron addition in the dentate gyrus (Imayoshi et al., 2008; Lagace et al., 2007; Ninkovic et al., 2007). Recently, permanent genetic fate mapping was established as a new strategy to monitor adult-generated neurons over long time frames (Mori et al., 2006; Ninkovic et al., 2007). Using this approach, distinct modes of neuron addition have been revealed for the major neurogenic zones of the adult brain (Ninkovic et al., 2007). In the dentate gyrus, adult neurogenesis contributed to only a minor fraction of the entire neuronal network in the granular cell layer.

Considering that in the epileptic brain seizures can increase neurogenesis on one hand and seizure-associated brain pathology can detrimentally affect neurogenesis on the other, we set out to analyze the long-term net impact in a chronic epilepsy model based on permanent genetic fate mapping. We have chosen the kindling model for the experiments for several reasons. In the kindling model, repetition of electrical stimuli induces seizures with a progressive increase in severity and duration (Loscher and Brandt, 2010). Once an animal exhibits generalized seizures in response to electrical stimulation, the heightened response is permanent, reflecting the generation of a hyperexcitable network in these kindled animals (McIntyre et al., 2002). To our great advantage the frequency of recurrent seizures can be controlled, so that we were able to compare the impact of different seizure history and seizure frequency on the long-term outcome of neurogenesis. In particular, we analyzed neuron addition in the dentate gyrus of kindled animals with and without further recurrent seizures in comparison with non-kindled, electrode-implanted control animals. Moreover, we compared the impact of a different seizure frequency in the chronic phase. The results are of particular interest in view of the ongoing debate about a functional impact of alterations in hippocampal neurogenesis on ictogenesis and epileptogenesis as well as psychiatric and cognitive co-morbidities (Danzer, 2012; Hattiangady and Shetty, 2008; Jessberger et al., 2007; Kokaia, 2011; Pekcec et al., 2008).

Material and methods

Animals

GLAST::CreERT2 mice (Mori et al., 2006) were crossed to CAG-CAT-eGFP mice (Kawamoto et al., 2000; Nakamura et al., 2006) to monitor newborn neurons using permanent genetic fate mapping. In the GLAST::CreERT2 mouse line the inducible form of Cre (CreERT2) expressed in the locus of the astrocyte-specific glutamate transporter (GLAST) allows for targeting of postnatal and adult neurogenesis at different stages with high efficiency as it originates from astroglial cells (Mori et al., 2006). In the CAG-CAT-eGFP mouse line, expression of enhanced green fluorescence protein (eGFP) is directed upon the Cre-mediated excision of the *loxP*-flanked CAT gene located between the modified chicken β-actin promoter with the CMVIE enhancer (CAG promoter) and the eGFP gene (Kawamoto et al., 2000). The fusion of Cre to the ligand binding domain of the modified estrogen receptor (ERT2) is restricted to the cytoplasm and translocates only upon tamoxifen stimulation into the nucleus where it can then mediate recombination (Feil et al., 1997; Mori et al., 2006). This allows us to mediate recombination at specific time points to target postnatally generated neurons in the neurogenic zones including newborn neurons of dentate gyrus (Mori et al., 2006). Previous studies demonstrated that following tamoxifen administration the stable expression of the reporter gene allows an efficacious monitoring of the progeny of cells that underwent recombination (Couillard-Despres et al., 2005; Kempermann et al., 2004; Mori et al., 2006; Ninkovic et al., 2007).

Prior to surgery, animals were housed in sibling groups under controlled environmental conditions (21–23 °C, 40–50% humidity, 12-h light/dark cycle) with free access to water and standard feed. To minimize the impact of circadian variations each procedure was performed at the same time each day in all experimental groups. Animals were housed separately during the period of experimentation.

Experimental procedures were performed according to the German Animal Welfare Act and were approved by the responsible governmental administration of Upper Bavaria.

Electrode implantation

For implantation of kindling electrodes, 62 GLAST::CreERT2 × CAG-CAT-eGFP male mice aged 10–16 weeks were anesthetized by intraperitoneal injection of 380 mg/kg chloral hydrate (Merck, Germany). A subcutaneous injection of bupivacaine 0.5% (Jenapharm, Germany) was applied for additional local anesthesia before exposure of the skull surface. The skull surface was exposed, and a bipolar electrode was implanted into the right hemisphere aimed at the amygdala using the following stereotaxic coordinates according to the atlas of Paxinos and Franklin (2004): +1.0 mm caudal, +3.2 mm lateral, +5.3 mm ventral (all respective to bregma). The electrodes consisted of two twisted Teflon-coated stainless steel wires (0.47 mm) separated by 0.55 mm at the tip. One screw, which served as the grounding electrode, was positioned over the left parietal cortex. Bipolar and ground electrodes were connected to plugs, and the electrode assembly and anchor screws were held in place with dental acrylic cement applied to the skull surface. Meloxicam (Boehringer Ingelheim, Germany) was administered as 1 mg/kg subcutaneous injection 30 min prior to the surgery and the administration was repeated 24 h later.

Tamoxifen administration

Tamoxifen (T-5648-5G, Sigma, Germany) was dissolved at 20 mg/ml in corn oil (63156, Fluka, Germany). Animals received intraperitoneal injections of 1 mg twice a day for five consecutive days following the first week of recovery from the surgery (Mori et al., 2006).

Amygdala kindling

Following a post-operative recovery period of 2 weeks, the pre-kindling afterdischarge threshold was determined by administering a series of stimulations (1 ms, monophasic square wave pulses, 50 Hz for 1 s) at intervals of 1 min increasing in steps of 20% of the previously applied current. The afterdischarge threshold was defined as the lowest current intensity discharges twice the pre-stimulation amplitude lasting at least 5 s. The next day, the initial kindling phase was started using an individual stimulation current 20% above the previously determined pre-kindling afterdischarge threshold. Stimulation of the amygdala was performed once daily (five times per week) for nine sessions. Following each stimulation, seizure severity, seizure duration and afterdischarge duration were measured. Seizure severity was scored according to Racine (1972): stage 1, immobility, eye closure, ear twitching, twitching of vibrissae, sniffing, facial clonus; stage 2, head nodding associated with more severe facial clonus; stage 3, clonus of one forelimb; stage 4, bilateral clonus of forelimbs; stage 5, generalized clonic seizures with rearing and falling. Once animals exhibit generalized seizures a stable hyperexcitable network has formed, which is associated with chronically enhanced seizure susceptibility and cellular and molecular alterations mimicking alterations in temporal lobe epilepsy (Goddard et al., 1969). Seizure duration was defined as the time period of limbic and/or motor seizure. Seizure severity and seizure duration were evaluated by an experimenter unaware of the animal's group

membership, and afterdischarge duration was recorded using an EEG. Cumulative afterdischarge duration was calculated as the sum of afterdischarge durations throughout the experiment.

Following the initial kindling phase, animals which exhibited at least one generalized seizure (bilateral forelimb clonus with or without rearing and loss of balance) towards the end of this phase were used for further investigations studying the impact of different seizure frequency during a chronic phase. For this purpose, animals were distributed homogeneously to three groups based on their afterdischarge threshold and the average of seizure severity during the initial kindling phase: one group was connected to the stimulating apparatus but did not receive any further stimulation (kindled/+0); the other two groups were stimulated once (kindled/+1) or three times (kindled/+3) per week for 12 weeks. Mice of the control group were also implanted and were handled the same way as kindled animals but did not receive electrical stimulations during the initial and chronic phase (electrode-implanted non-kindled control group). The experimental design is depicted in Fig. 1A.

BrdU treatment

To study cell proliferation in the chronic phase following the initial kindling phase we used the thymidine analog 5′Bromodeoxyuridine (BrdU). The purpose of BrdU application was to study proliferation changes after the formation of a hyperexcitable network. BrdU is incorporated into the DNA during the S phase of the cell cycle and is available for about 15 min following injection and thus labels the proportion of dividing cells that are in the DNA-synthetic phase of the cell cycle during this period (Mandyam et al., 2007). Control and kindled mice received a total of eight intraperitoneal injections of 50 mg/kg BrdU (Sigma, Germany) during a four-week period (Fig. 1A). Each week animals received a BrdU injection following the stimulation session (note that the control and kindled/+0 groups were only connected to the stimulator but did not receive electrical current) and 8 h later they received the second administration of BrdU.

PCR genotyping

Mouse tail DNA was used for PCR genotyping before and after the experiments.

The following primers were used for GLAST::CreERT2 genotyping:

GLAST F8 (5′-GAGGCACTTGGCTAGGCTCTGAGGA-3′),
GLAST R3 (5′-GAGGAGATCCTGACCGATCAGTTGG-3′),
CER1 (5′-GGTGTACGGTCAGTAAATTGGACAT-3′).

Only heterozygous GLAST::CreERT2 mice were used for the experiment to exclude functional defects from lack of GLAST function. So far no defects have been observed in mice with only one functional allele for GLAST (Mori et al, 2006).

For CAG-CAT-eGFP genotyping AG2 (5′-CTGCTAACCATGTTCATGCC-3′) and CAT-2 (5′-GGTACATTGAGCAACTGACTG-3′) were used.

Tissue preparation

At the end of the experiment (16 weeks after surgery), mice were deeply anesthetized with chloral hydrate (Applichem, Germany) and were transcardially perfused with 0.01 M phosphate buffered saline followed by 4% paraformaldehyde. The brains were removed and transferred into 30% sucrose and stored at 4 °C. Five series of 40 µm coronal sections of cerebrum were cut using a Reichert–Jung 1205 freezing microtome. Sections were stored at −80 °C in cryoprotecting solution (glycerol and 0.2 M phosphate buffer, pH 7.4, 1:1 in volume).

Fifteen animals were excluded from the experiment for different reasons including lack of behavioral and electrographic seizure induction during initial threshold determination, loss of the electrode during the experiment, general health disturbance and unsuccessful recombination. Six animals did not show generalized seizures during the initial kindling phase and therefore were not included in the final combination of groups.

Seven mice from each group were chosen randomly for counting purposes. The proportion of new granule cells among all granular cells was determined in four animals per group.

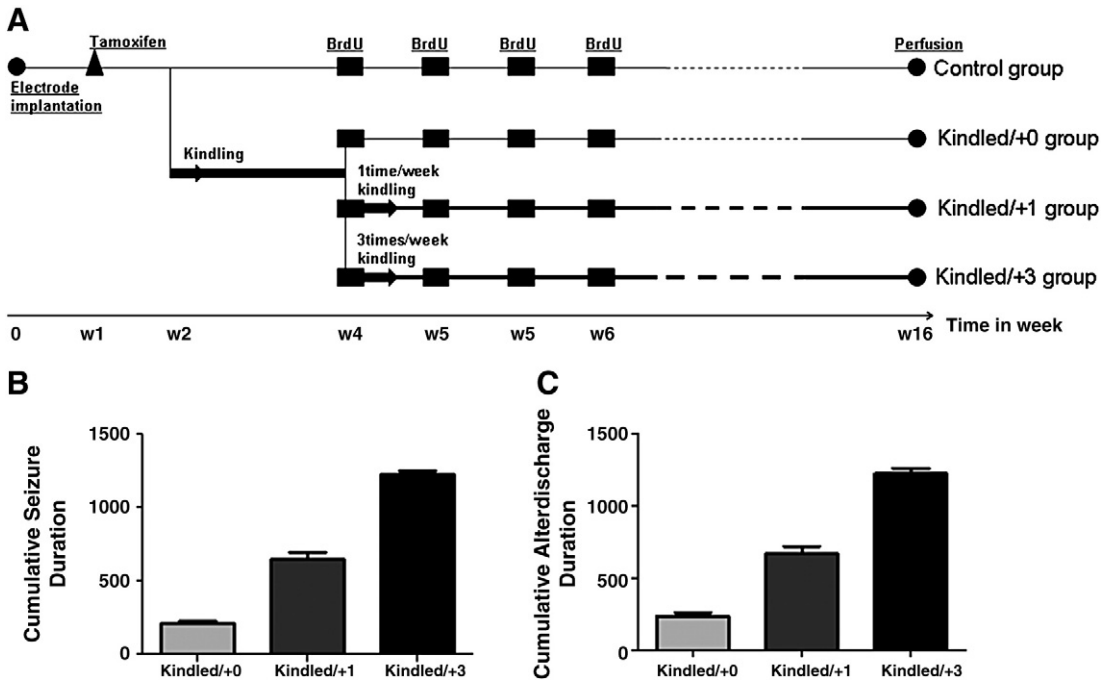

Fig. 1. Kindling data. A: Experimental design including project planning and stimulation protocols. B: Cumulative seizure duration reflects the difference of stimulation protocols between groups. C: Cumulative afterdischarge duration reflects the difference of stimulation protocols between groups. Data are given as mean ± SEM. Significant differences are found between all of the groups. (One-way ANOVA test, $p<0.05$).

BrdU/NeuN double-labeling

Free-floating sections were rinsed in 0.05 M Tris-buffered saline (TBS) and incubated in formamid (Sigma, Germany) for 2 h at 65 °C. Then sections were incubated in 2 N HCl for 30 min at 37 °C and washed in 0.1 M borate buffer (pH 8.5) for 10 min. Blocking was performed by using donkey serum. Sections were then incubated in an antibody mixture containing rat anti-BrdU (AbD Serotec, UK), 1:30, and mouse anti-NeuN (Chemicon, Germany), 1:500, at 4 °C overnight. After washing the sections, carbocyanin-3-labeled donkey anti-rat antibodies (Jackson Immunoresearch Laboratories, USA; 1:1000) and biotinylated donkey anti-mouse antibodies (DAKO, Germany; 1:500) were applied for 60 min. The sections were washed again and incubated in carbocyanin-2-labeled streptavidin (Jackson Immunoresearch Laboratories, USA), 1:2000, for 60 min. Finally, all sections were washed, mounted onto glass slides, air dried, dehydrated, and cover-slipped with Entellan (Merck, Germany).

BrdU/GFAP double-labeling

Pre-treatment was performed as described above. Primary antibodies mixture contained rat anti-BrdU (AbD Serotec, UK; 1:300) and mouse anti-GFAP (Millipore, Germany; 1:500). Cy3-labeled donkey anti-rat antibody (Jackson Immunoresearch Laboratories, USA; 1:1000) and Alexa 647 donkey anti-mouse (Jackson Immunoresearch Laboratories, USA; 1:1000) were used for detection. Cover-slipping was performed as described above.

eGFP/NeuN double-labeling

After washing with TBS and blocking with goat serum, all sections were treated with the mixture of primary antibodies chicken anti-eGFP (Aves, USA; 1:500) and biotinylated mouse anti-NeuN (Chemicon, Germany; 1:300) at 4 °C overnight for double-labeling of eGFP and neuronal nuclei protein (NeuN). Following washing, DyLight488 goat anti-chicken (Dianova, Germany; 1:200) and Cy3-streptavidin (Dianova, Germany; 1:1000) were applied for 60 min. Cover-slipping was performed as described above.

eGFP/Prox1 double-labeling

In order to confirm hilar ectopic neurons, additional animals from the kindled/+3 group were used to perform eGFP/Prox1 staining. Primary antibodies mixture consisted of chicken anti-eGFP (Aves, USA; 1:500) and rabbit anti-Prox1 (Covance, US; 1:500). These antibodies were detected using DyLight488 goat anti-chicken (Dianova, Germany; 1:1000) and biotinylated goat anti-rabbit (Dianova, Germany; 1:1000) and Cy3-streptavidin (Dianova, Germany; 1:1000). Cover-slipping was performed as described above.

eGFP/DCX double-labeling

The primary antibodies mixture consisted of chicken anti-eGFP (Aves, USA; 1:500) and guinea pig anti-DCX (Chemicon, Germany; 1:1000). These antibodies were detected by using DyLight488 goat anti-chicken (Dianova, Germany; 1:250) and Cy3 goat anti-guinea pig (Jackson Immunoresearch Laboratories, USA; 1:500). Cover-slipping was performed as described above.

eGFP/Ki67/GFAP triple-labeling

Due to the limit of available tissue, eGFP/Ki67/GFAP were stained in the same sections but analyzed separately (eGFP/Ki67 and eGFP/GFAP). The primary antibodies mixture consisted of chicken anti-eGFP (Aves, USA; 1:500), rabbit anti-Ki67 (Abcam, UK; 1:500) and mouse anti-GFAP (Millipore, Germany; 1:500). These antibodies were detected using DyLight488 goat anti-chicken (Dianova, Germany; 1:1000), biotinylated goat anti-rabbit (Dianova, Germany; 1:1000) and Cy3-streptavidin (Dianova, Germany; 1:1000), and Alexa 647 donkey anti-mouse (Jackson Immunoresearch Laboratories, USA; 1:1000) respectively.

Quantification and image analysis

Counting for double-labeling of cells with neuronal markers was performed in five brain sections in both left and right dentate gyrus. The sections were spaced 200 μm apart. Cell counts of fluorescent signals cells were performed in an area encompassing the entire dentate granule cell layer (upper and lower blades) and extending approximately two cell body widths deep into the hilus. The hilus was defined as the inner border of the granule cell layer and two straight lines connecting the tips of the granule cell layer and the proximal end of the CA3 region. Immunoreactive cells were counted on a computer monitor to improve visualization using a Hitachi HV-C20A (Hitachi, Japan) digital camera connected to a Zeiss LSM 510 microscope (Carl Zeiss, Germany). The signal of the fluorescent labeling was captured with the StereoInvestigator 6.0 (Microbrightfield Europe, Germany). Double-labeling was verified by careful analysis of the confocal z-series of multiple cells in each animal.

Proportions of eGFP-positive cells among NeuN-positive cells were assessed in the aforementioned double-labeling counting areas using an unbiased random systematic sampling method. Three 30×30 μm counting frames were applied on the upper and lower blades of the DG on both sides (60 counting boxes per animal). Sampling area was optically sectioned using 3 μm Z-intervals in 9 μm of depth. Cells which were located in the lookup section or were in contact with the exclusion lines were not counted. At least 400 NeuN-positive cells were counted in each animal.

To confirm successful recombination, two animals were selected from each group and DCX-positive cells were counted in two hippocampal regions with a distance of 200 μm. The proportion of eGFP-positive newly generated neurons co-labeled with DCX indicated the efficacy of recombination.

Confocal images were further improved for color correction by using Irfanview 4.28 (http://www.irfanview.com/).

Statistics

Statistical analyses were performed using Prism software (GraphPad; version 5.0). Data were analyzed using One-way ANOVA followed by Tukey's post-hoc test, when appropriate. The Pearson's correlation coefficient was used to test for a correlation between the kindling data and the number of counted cells. The Student's paired *t*-test was used to compare counted numbers of left and right hemispheres and no significant difference was found in any of the quantifications. Data are expressed as mean ± SEM. A value of $p < 0.05$ was considered significant. All tests were used two-sided.

Results

Kindling data

Fully kindled animals were distributed homogenously to the different groups for the chronic phase. Statistical comparison of seizure data from the initial kindling phase confirmed that groups did not differ in the initial afterdischarge threshold ($p = 0.40$) and in the mean seizure severity ($p = 0.83$) during the first 10 stimulation sessions.

In the chronic phase, animals which were stimulated once per week exhibited a mean seizure severity of 4.29 ± 0.39, i.e. generalized seizures were observed during the majority of stimulation sessions. Mice which received three stimulations per week exhibited a mean

seizure severity of 4.62 ± 0.16 during the chronic phase, i.e. generalized seizures were observed during the majority of stimulation sessions.

In accordance with the project planning and the stimulation protocols (Fig. 1A), the average cumulative seizure duration and afterdischarge duration differed between the groups: kindled/+0 group showed an average cumulative seizure duration of 210.29 ± 16.82 s and an average cumulative afterdischarge duration of 234.00 ± 72.27 s. The respective data for the kindled/+1 group were 646.86 ± 48.25 s and 668.57 ± 52.79 s, and for the kindled/+3 group 1225.00 ± 26.59 s and 1223.14 ± 37.61 s, respectively (Fig. 1B, C).

All the above mentioned data have been determined for the animals that were randomly selected for immunohistological studies (n = 7 in all groups).

Hippocampal cell proliferation and neurogenesis during the early chronic phase

Double-labeled eGFP/Ki67 cells (Fig. 3A, B) were quantified in the subgranular proliferation zone of all animals (control: 21.29 ± 3.20, kindled/+0: 23.43 ± 2.36, kindled/+1: 23.43 ± 5.83, kindled/+3: 22.71 ± 3.95) (Fig. 4A). Statistical analysis did not show any significant difference between the groups (p = 0.98).

BrdU-labeled cells were detected in the subgranular proliferation zone and the granule cell layer in all groups (control: 21.29 ± 3.76, kindled/+0: 141.70 ± 33.20, kindled/+1: 138.00 ± 29.34, kindled/+3: 159.7 ± 31.79). As mentioned before, BrdU administration was performed following the initial kindling phase during the first 4 weeks of the chronic phase. During this period the control and kindled/+0 groups had no seizures and 4 or 12 seizures occurred in the kindled/+1 and kindled/+3 groups, respectively. All groups of kindled mice exhibited a significant increase of 6.5 to 7.5 fold in the number of BrdU-positive cells, exceeding that in control animals. Interestingly, the degree of increase was comparable in animals not receiving further stimulations and in animals with ongoing repeated seizures (Fig. 2A).

Neuronal differentiation of surviving cells generated during the phase of BrdU administration was assessed based on BrdU/NeuN double-labeling (Fig. 2B, 3C–E). All groups of kindled mice exhibited an increase in the number of newborn neurons during the chronic phase in comparison to the control animals which reached a significant difference in kindled/+3 group (kindled/+0: 3.9 fold, kindled/+1: 4.6 fold and kindled/+3: 7.7 fold). While weekly single additional seizures did not further increase the number of newborn neurons, the elicitation of three seizures per week during the chronic phase further enhanced the rate of hippocampal neurogenesis resulting in a number of BrdU/NeuN double-labeled cells which significantly exceeded that of non-kindled animals (control: 6.57 ± 1.46, kindled/+0: 25.86 ± 7.53, kindled/+1: 30.00 ± 7.59, kindled/+3: 50.71 ± 7.76; p = 0.04) (Fig. 2B).

Considering data from all kindled animals, the number of double-labeled cells correlated with the cumulative duration of afterdischarges and seizure duration (Pearson's correlation coefficients 0.53 and 0.51; p = 0.01 and 0.02, respectively) (Fig. 2C).

Double-labeling the BrdU-positive cells with anti-glial fibrillary acidic protein (GFAP) proved the presence of astrocytes mostly in the subgranular zone in all groups; however the visual inspection indicated no obvious differences in the number of cells between groups (Fig. 3O, P).

Long-term monitoring of kindling effects on hippocampal neurogenesis

There were eGFP-positive cells present in all of the animals which demonstrated successful recombination in all groups (Fig. 3F–I).

The number of recently born neuronal progenitor cells and early post-mitotic neurons was assessed based on counting of cells expressing both DCX and the reporter eGFP (Fig. 3J, K). One animal of the kindled/+0 group demonstrated to be an outlier due to an extremely high number of eGFP/DCX-labeled cells (335 positive cells). According to the three-sigma rule this animal was not considered in the statistical analysis.

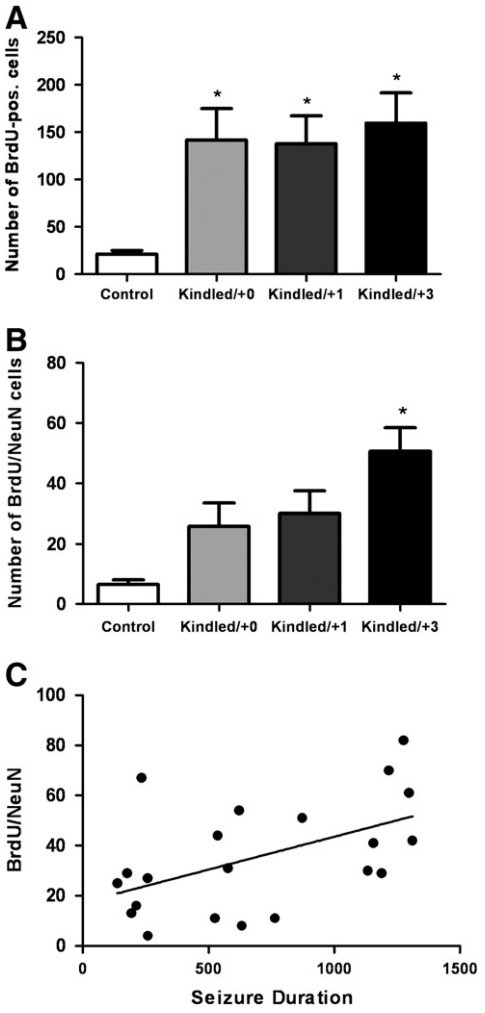

Fig. 2. Hippocampal cell proliferation and neurogenesis during the early chronic phase. A: Analysis of BrdU-positive cells in the dentate gyrus showed a 6.5 to 7 fold increase in all kindled groups. B: Neuronal differentiation was assessed based on analysis of BrdU/NeuN double-labeled cells in the dentate gyrus. The previous kindling procedure resulted in an induction of hippocampal neurogenesis which was enhanced with elicitation of three seizures per week, but not with single additional seizures. C: The number of BrdU/NeuN-positive cells showed positive correlation with cumulative seizure duration. Data are given as mean ± SEM. Significant differences are indicated by asterisks (kindled groups vs. control group). (One-way ANOVA test, $p<0.05$; Pearson's correlation coefficient = 0.51, p = 0.02).

The proportion of eGFP-positive newly generated neurons reached a stable number of 83.19 ± 3.96% of all DCX-labeled cells 15 weeks after the induction of recombination. This number is close to the quantification of β-gal reporter (around 90%) 1.5 and 9 months after induction in the GLAST::CreERT2/R26R mouse line reported by Ninkovic et al. (2007). Therefore our data demonstrate a very efficient labeling of neuronal progenitor cells in the subgranular zone.

Analysis of eGFP/DCX-labeled cells did not show any significant difference between the groups (p = 0.06).

Careful attention was paid to the presence of hilar basal dendrites in multiple eGFP-positive cells from all groups. However, our analysis did not reveal a relevant persistence of these formations in our model.

Based on cell counts of eGFP/NeuN-labeled cells (Fig. 3L–N), information was obtained about the generation of newborn neurons during the complete experimental time frame beginning after tamoxifen administration, i.e. consisting of the initial kindling phase and the chronic phase. It is important to note that recombination does not take place in

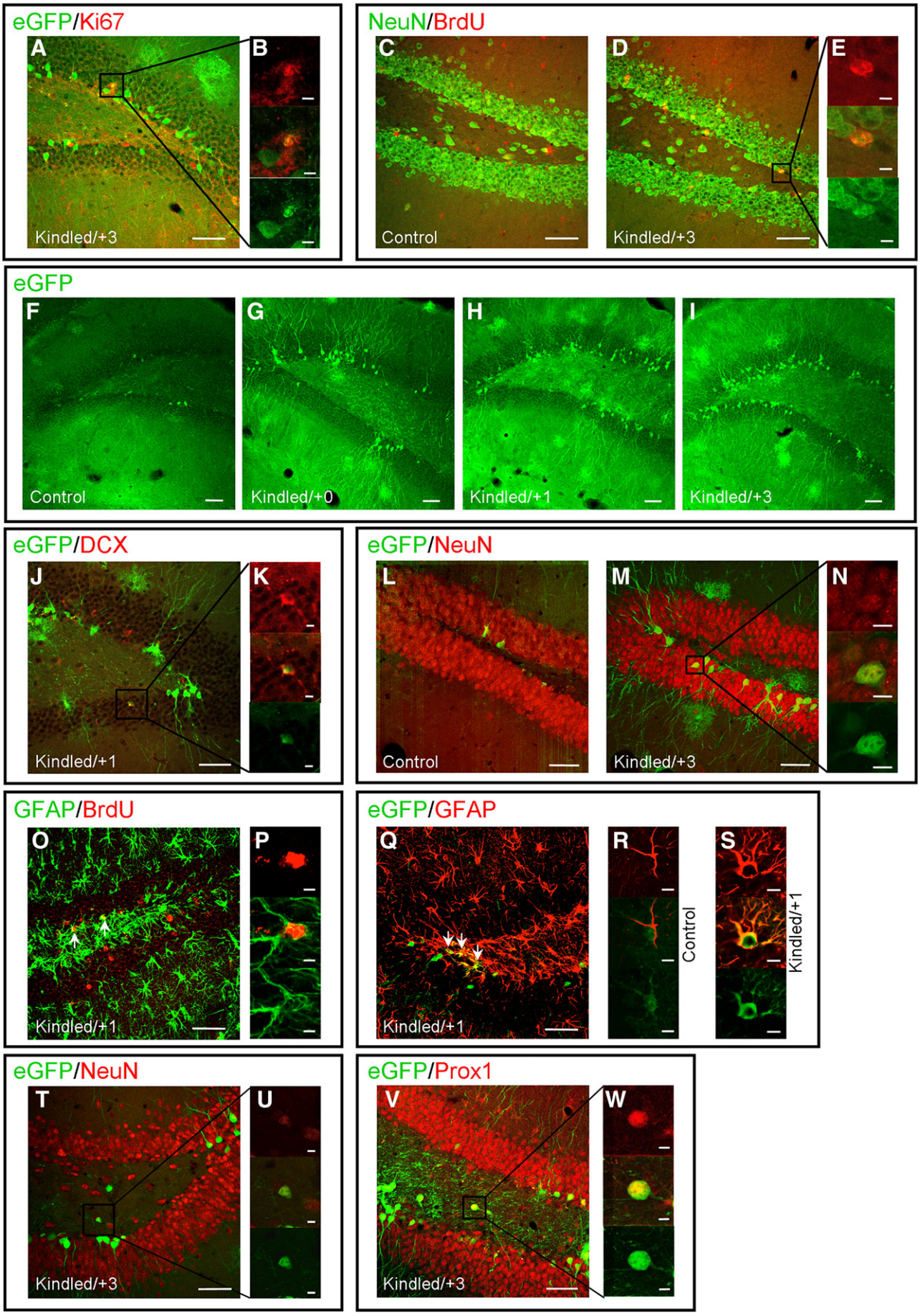

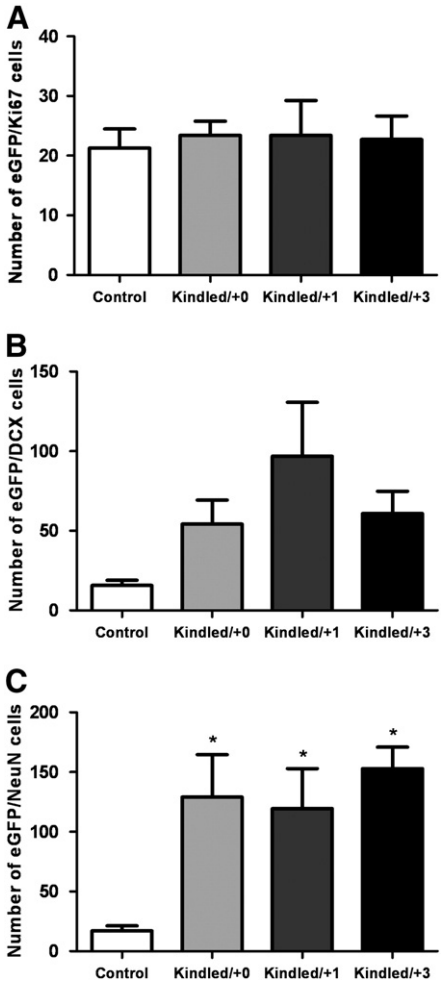

Fig. 4. Long-term monitoring of kindling effects on the hippocampal neurogenesis. A: Analysis of eGFP/Ki67 double-labeled cells in the dentate gyrus showed no difference of proliferation between the groups. B: Analysis of eGFP/DCX double-labeled cells in the dentate gyrus did not reveal any significant difference among different groups. C: Analysis of eGFP/NeuN double-labeled cells in the dentate gyrus gives information about the generation of newborn neurons during complete experimental time frame. Data are given as mean ± SEM. Significant differences are indicated by asterisks (kindled groups vs. control group). (One-way ANOVA test, $p<0.05$).

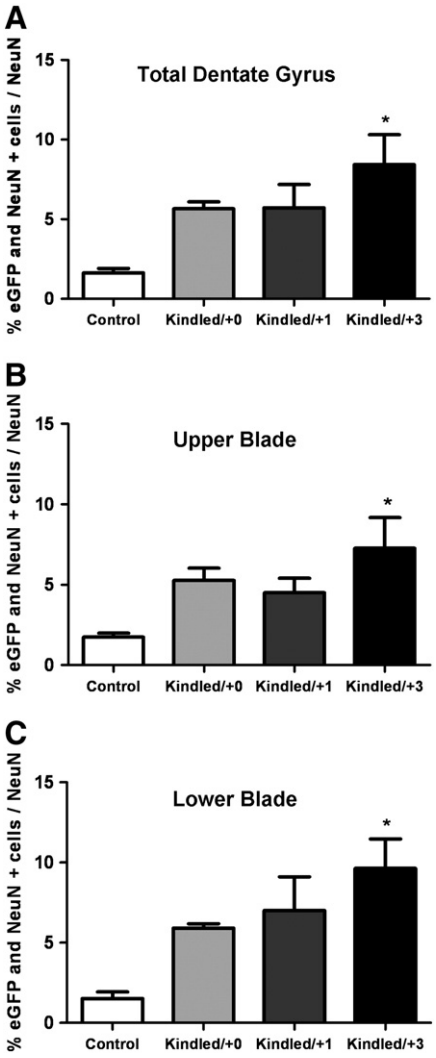

Fig. 5. Relative portion of newborn neurons among all granule cells. A: Proportion of eGFP/NeuN double-labeled cells among all NeuN cells in the counted frames of dentate gyrus was significantly increased in kindled groups with further stimulations. B: Proportion of eGFP/NeuN double-labeled cells among all NeuN cells in the counted frames of the upper blade was higher in the kindled/+3 group. C: Proportion of eGFP/NeuN double-labeled cells among all NeuN cells in the counted frames of the lower blade of the dentate gyrus was higher in the kindled/+3 group. Data are given as mean ± SEM. Significant differences are indicated by asterisks (kindled groups vs. control group). (One-way ANOVA test, $p<0.05$).

adult neurons, therefore all eGFP/NeuN-labeled cells are newly generated neurons following tamoxifen administration.

No double-labeled cells were identified in the hilus of the control group, the kindled/+0 and the kindled/+1 group. In contrast, the majority of mice from the kindled/+3 group exhibited single newborn neurons located in the hilus expressing both NeuN and the reporter eGFP (Fig. 3T, U). These cells proved to be ectopic granular cells based on a double-labeling of eGFP/Prox1 (Fig. 3V, W). In none of the groups were eGFP/NeuN-labeled cells evident in the molecular layer. In all groups eGFP/NeuN-labeled cells were identified in both blades of the dentate gyrus with most cells being located in the half of the cell layer adjacent to the hilus (Fig. 3L, M). Thus, as previously shown by Ninkovic et al. (2007) and Lagace et al. (2007), the majority of the new cells did not migrate far into the granule cell layer before becoming integrated.

The number of eGFP/NeuN-labeled cells in the granule cell layer was significantly increased in all kindled groups (control: 17.14 ± 4.03; kindled/+0: 129.1 ± 35.51; kindled/+1: 119.40 ± 33.48; kindled/+3: 152.9 ± 17.98). Interestingly, the number of newborn neurons did not

Fig. 3. Fluorescence micrographs. A: eGFP (green) and Ki67 (red) immunostaining in kindled/+3 group. B: High magnification of an eGFP/Ki67-labeled cell. C: BrdU (red) and NeuN (green) immunostaining in control group. D: BrdU/NeuN immunostaining in kindled/+3 group. E: High magnification of a double-labeled BrdU/NeuN subgranular neuron. F–I: eGFP (green) immunostaining in all four groups. J: eGFP (green) and DCX (red) immunostaining in kindled/+1 group (no significant difference in double-labeling seen between all four groups). K: High magnification of a double-labeled eGFP/DCX newborn neuron. L: eGFP (green) and NeuN (red) immunostaining in control group M: eGFP/NeuN immunostaining in kindled/+3 group. N: High magnification of a double-labeled eGFP/NeuN neuron. O: GFAP (green) and BrdU (red) immunostaining is shown in an animals from kindled/+1 group. No difference was observed between the groups. Arrows show several double-labeled cells in subgranular zone. P: High magnification of a double-labeled GFAP/BrdU cell. Q: eGFP (green) and GFAP (red) immunostaining in animal from kindled/+1 group. Arrows show several double-labeled cells in subgranular zone. R: High magnification of a double-labeled eGFP/GFAP astrocyte in control group. S: High magnification of a double-labeled eGFP/GFAP reactivated astrocyte in kindled/+1 group. Hypertrophic astrocytes were observed in all kindled groups. T: Ectopic hilar neurons were found in kindled/+3 group using eGFP/NeuN staining. U: High magnification of an eGFP/NeuN double-labeled ectopic hilar neuron. V: eGFP (red) and Prox1 (green) immunostaining shows ectopic hilar neuron in kindled/+3 group. W: High magnification of an eGFP/Prox1 ectopic hilar neuron. Scale bar is 5 μm in high magnification micrographs (B, E, K, N, P, R, S, U, W) and 50 μm in the rest of the images.

differ between kindled mice without additional seizures and mice with 12 or 36 seizures during the chronic phase (Fig. 4C).

Addressing the question of how alterations in cell proliferation and neurogenesis affect the relative portion of newborn neurons among all granule cells, we used an unbiased random sampling method to count the eGFP/NeuN cells among those NeuN-labeled. The total number of NeuN-positive cells did not differ between groups (control: 439.30 ± 11.11, kindled/+0: 478.8 ± 6.69, kindled/+1: 456.6 ± 12.98, kindled/+3: 444.3 ± 13.76; $p = 0.1$).

The percentage of reporter positive cells among the granule cells reached significantly higher levels in the kindled/+3 group as compared to non-kindled controls ($p = 0.01$). The same result was confirmed in both upper and lower blades of dentate gyrus ($p = 0.03$ and $p = 0.01$, respectively) (Fig. 5B, C).

Double-labeling of eGFP positive cells with GFAP marker proved a difference in morphology of astrocytes in kindled groups in comparison to the control. Reactive astrocytes were detected in the kindled groups with an increase in length and width of processes (Fig. 3Q–S).

Discussion

Genetic fate mapping analysis in the mouse amygdala kindling model revealed that recurrent seizures exert an impact on the long-term balance with a net effect on the cellular composition of the granule cell layer.

Analysis of the number of adult-generated reporter-positive neurons during the complete kindling procedure demonstrated a significant increase regardless of the seizure density and the cumulative number of seizures. Interestingly, alterations were also evident in animals which were kindled to generate a hyperexcitable network but did not experience any further seizures. Although the exact functional significance of an increase in adult-generated granule cells remains to be further explored, it is considered rather likely that pronounced alterations in the rate of hippocampal neurogenesis should have functional implications for the course and consequences of epilepsy (Danzer, 2012; Kokaia, 2011; Parent and Murphy, 2008). In view of the present proof of lasting changes in the makeup of the granule cell layer despite lack of recent seizures, these functional implications might even apply to cases with long intervals between seizure events. Previously, Coras and colleagues have shown in ex vivo studies that a longer duration of seizures does not affect neurogenesis in human patients (Coras et al., 2010). Our experiments support this finding for the first time in an animal model.

Earlier studies have already compared the impact of a different number of seizures in the kindling model (Fournier et al., 2010; Parent et al., 1998). Parent et al. (1998) described that 4–6 generalized seizures did not affect hippocampal cell proliferation and neurogenesis, whereas increased dentate granule cell neurogenesis was evident in groups experiencing 9–10 or 19–20 generalized kindled seizures. In contrast, genetic fate mapping in the present study revealed that nine kindling stimulations with a mean number of 4.7 ± 1.13 (mean ± SEM) generalized seizures are sufficient to cause lasting changes in the composition of the granule cell layer. The discrepancy to the previous findings underlines the advantages of permanent genetic fate mapping approaches. BrdU is incorporated during a short time span following its injection, so that even repeated BrdU injections will label only a minor fraction of newborn cells (Taupin, 2007a). Therefore, analysis of BrdU-labeled cells can result in an underestimation of hippocampal neurogenesis and the extent of its modulation (Imayoshi et al., 2008; Lagace et al., 2007; Ninkovic et al., 2007).

Whereas analysis of the number of adult-generated neurons introduced during the complete time span following implantation did not reveal any impact of the cumulative number of seizures or seizure frequency, differences in neurogenesis were evident based on BrdU/NeuN labeling during the first 4 weeks of the chronic phase, i.e. after the animals acquired a generalized-state. The number of newborn neurons generated during this phase reached a significant difference only in animals with a high seizure density in comparison to the control group. In contrast, hippocampal cell proliferation rates analyzed based on eGFP/Ki67 double-labeling did not differ by the end of the experiment among the groups. In the early chronic phase, cell proliferation proved to be enhanced in a comparable manner regardless of the occurrence of additional seizures and their number.

Looking at previous studies indicates that controversial findings have been obtained regarding the impact of chronic recurrent seizures in both kindling and post-status epilepticus models. Recently, Fournier et al. (2010) described that short-term kindling with 30 electrical stimulations increased the number of immature neurons, whereas long-term kindling with 99 electrical stimulations did not. The differences to our results might be related to higher seizure density and the fact that conclusions in their study were merely based on doublecortin analysis. In post-status epilepticus models with chemical induction of status epilepticus a long-term decline in hippocampal neurogenesis has been repeatedly reported (Hattiangady and Shetty, 2008; Hattiangady et al., 2004). Recent findings revealed that decreased neuronal differentiation underlies this reduction in hippocampal neurogenesis (Hattiangady and Shetty, 2010). Thus, chemically-induced status epilepticus seems to result in anti-neurogenic long-term conditions which modulate neuronal fate-choice decision. This effect might be related to the pronounced pathology occurring as a consequence of chemically induced status epilepticus (Loscher and Brandt, 2010). In support of this hypothesis, we did not observe a respective decline in neurogenesis in a model with electrically-induced status epilepticus which is associated with milder pathological alterations (Pekcec et al., 2008; Seeger et al., 2011). Thus, recurrent seizures in the chronic phase might actually be pro-neurogenic. However, the effect can be masked or counteracted by anti-neurogenic conditions related to pathological alterations affecting the neurogenic niche such as inflammatory events.

As emphasized by Meltzer et al. (2005), the integration of new neurons into adult neural circuits can promote or impair circuit function depending on whether homeostatic mechanisms are in place to regulate the resulting changes in neural activity. In line with this statement, there is concern about detrimental long-term consequences of seizure- and epilepsy-associated alterations in the generation of new neurons (Danzer, 2012; Kokaia, 2011; Parent and Murphy, 2008). So far the long-term net effect of seizure-associated alterations has remained an open question. Permanent genetic fate mapping now rendered information about the impact of recurrent seizures on the relative contribution of newborn neurons to the dentate gyrus. Whereas the initial kindling phase and low intensity stimulation of one seizure per week did not significantly affect the relative portion of new neurons among all dentate granule cells, additional recurrent seizures resulted in an expansion of the fraction of new granule cells. Thus, repeated seizure activity seems to disturb the homeostatic mechanisms of granule cell turnover rates with a shift towards integration of new cells vs. cell loss. A disturbance of homeostasis in the granule cell layer via an increased percentage of new cells might result in different functional consequences. Each new excitatory neuron will probably add excitatory drive affecting dentate gyrus outputs (Meltzer et al., 2005). As Meltzer et al. (2005) discussed, memory recall might be impaired related to erroneous recruitment of output cells if a given memory depends on activation of a precise pool of hippocampal neurons. In line with this hypothesis, data from animals indicate that recall of older memories benefits from a reduction in neurogenesis (Feng et al., 2001). Moreover, we already reported that partial normalization of hippocampal neurogenesis in a rodent epilepsy model improves spatial learning (Pekcec et al., 2008). Thus, the excessive addition of new neurons seems to disturb hippocampal neuronal circuits involved in information processing and might hamper subsequent integration of further newborn neurons. This may impact memory formation that is discussed to involve the integration of new neurons into hippocampal networks (Wiskott

et al., 2006). Moreover, studies on human patients with temporal lobe epilepsy suggest that neuronal density in the internal limb of the dentate gyrus (anatomically comparable to the lower blade of the dentate gyrus in rodents) is an important predictor for the patient's capability to store and recall declarative memory (Pauli et al., 2006). Therefore, alterations in the proportion of new granule cells might contribute to epilepsy-associated cognitive deficits.

Regarding a putative role of adult-generated neurons in ictogenesis and epileptogenesis, controversial findings have been reported, thereby hindering the development of clear-cut conclusions. In general, the addition of excitatory cells suggests an increase in excitability. However, it has been reported that newborn granule cells that integrate into the granule cell layer of epileptic animals are less excitable and have fewer dendritic spines than cells from control animals (Jakubs et al., 2006; Murphy et al., 2011; Wood et al., 2011). Thus, variations in morphological development of adult-generated granule cells might help to maintain homeostasis and might prevent an excessive increase in dentate gyrus excitability in the epileptic brain (Danzer, 2012). In support of this concept, various studies indicated that modulating neurogenesis in different epilepsy models has no relevant and consistent effects on seizure development (Danzer, 2012; Kokaia, 2011; Pekcec et al., 2007; Pekcec et al., 2008; Pekcec et al., 2011). Considering these data, an increase in the fraction of newborn cells might not affect ictogenesis and epileptogenesis.

In contrast, ectopic granule cells in the hilus exhibit bursting behavior and a higher ratio of excitatory inputs to inhibitory inputs (Scharfman et al., 2000; Zhan et al., 2010). The fact that reporter-positive ectopic neurons in the hilus only occurred in kindled animals with high seizure frequency suggests that these cells are not critical for kindling development. However, considering that these can develop with a glutamatergic granule cell phenotype (Scharfman and McCloskey, 2009) they might contribute to disease severity in individuals with a high seizure density.

Several studies suggest that astrocytes play a key role in epilepsy development through various mechanisms (Arisi et al., 2011; Seifert et al., 2010; Tian et al., 2005). Kindling-induced seizures have been shown to result in prominent cytoskeletal changes in astrocytes which take place early in the development of kindling and persist for long periods of time (Khurgel and Ivy, 1996). On the other hand, it has been shown that altered neurogenesis in epileptic animals changes the one-to-one relationship between astrocytes and newly born granule cells (Shapiro and Ribak, 2005), which may contribute to a hyperexcitable condition by making the new born neurons more susceptible to aberrant synaptic targeting (Arisi et al., 2011). Reactive astrocytosis involves an increase in the size of the soma as well as in the length and width of astrocytic processes which are indicative of hypertrophy and is occasionally accompanied by proliferation of these cells (Khurgel and Ivy, 1996; Rogawski, 2005). Hattiangady and Shetty (2010) showed that in a chronic kainic acid-induced status epilepticus in rats, differentiation of newly born cells into S-100ß positive astrocytes increased in epileptic animals in comparison to the controls. On the other hand, in a kindling model of aged rats, Arisi et al., (2011) reported an increased volume and activated morphology of astrocytes in the kindled group but no quantitative difference of GFAP positive cells in the hilus and CA1. As Hawrylak et al. (1993) point out, this might be due to the fact that it is unlikely to see astrocytic proliferation in the kindling model in a region distant from the implantation site (Hawrylak et al., 1993). Our results from double-labeling the proliferative cells in the chronic phase with the astrocytic marker GFAP, proved the presence of astrocytes in all of the animals especially in the subgranular area. However, we did not observe any major difference in the number of these cells between the groups through our visual observation. Using an eGFP/GFAP staining, we confirmed astrocytic identity of cells in the subgranular zone similar to the findings of Mori et al. (2006) in GLAST::CreERT2–Cx43::LacZ mice. We could see hypertrophic astrocytes in all of the kindled groups but not in the controls. Therefore, our model suggests that seizures result in structural changes of astrocytes that are detectable long after the termination of these insults.

Regarding the homogeneity in the number of BrdU-labeled cells among kindled animals and the differences between BrdU/NeuN-labeled cells, it needs to be considered that the formation of other types of glial cells, i.e. microglia and oligodendrocytes can also be enhanced in epilepsy models (Hattiangady and Shetty, 2010; Vezzani et al., 2011). Hattiangady and Shetty (2010) reported that $NG2^+$ oligodendrocyte progenitors and S100beta-positive astrocytes increased in a chronic rodent model of temporal lobe epilepsy. In addition, microglia cell proliferation as well as migration of bone marrow cells into the brain can occur in the chronic epileptic brain (Longo et al., 2010; Vezzani et al., 2011), and might, thus, have contributed to the number of BrdU labeled cells. In this context, it is of particular interest that Hattiangady and Shetty (2010) have concluded that diminished dentate granule cell neurogenesis in chronic temporal lobe epilepsy is linked to a dramatic decline in the neuronal fate-choice decision of newly generated cells with newly born cells mainly turning into glia. The fact that we did not observe any major alterations in the number of astrocytes might be related to the use of another astrocytic marker or to differences between the animal models used. Future investigations will be necessary to determine to which extent the other cell types mentioned above have contributed to the overall number of new cells in the chronic kindling paradigm used in the present study.

Conclusion

Genetic fate mapping analysis demonstrated that recurrent seizures result in a lasting change in the makeup of the granule cell layer with alterations in the relative contribution of newborn neurons to the granule cell network. Interestingly, the formation of a hyperexcitable network and a prior seizure history without recent seizure activity can result in pronounced long-term alterations regarding the absolute number of new granule cells. However, seizure density also seems to play a critical role with more frequent seizures resulting in increased portions of new neurons.

In future studies it is of interest to use the genetic fate mapping approach to further study electrophysiological properties of newly generated and integrated neurons in the kindling model as well as functional consequences with respect to memory impairment in a hippocampal kindling paradigm.

Acknowledgments

This research was supported by a grant of the Deutsche Forschungsgemeinschaft (DFG for 1103 PO-681/5-1; SFB 870). The authors thank Andreas Blutke for his valuable comments regarding the counting methods. We would like to thank Carmen Mayer, Heidrun Zankl, Marion Fisch and Angela Vicidomini for their technical assistance and Anton Pekcec for his contributions to the initial planning phase. In addition we thank Hannes Wendt for the help during electrode implantations.

References

Arisi, G.M., Ruch, M., Foresti, M.L., Mukherjee, S., Ribak, C.E., Shapiro, L.A., 2011. Astrocyte alterations in the hippocampus following pilocarpine-induced seizures in aged rats. Aging Dis. 2, 294–300.

Cha, B.H., Akman, C., Silveira, D.C., Liu, X., Holmes, G.L., 2004. Spontaneous recurrent seizure following status epilepticus enhances dentate gyrus neurogenesis. Brain Dev. 26, 394–397.

Coras, R., Siebzehnrubl, F.A., Pauli, E., Huttner, H.B., Njunting, M., Kobow, K., et al., 2010. Low proliferation and differentiation capacities of adult hippocampal stem cells correlate with memory dysfunction in humans. Brain 133, 3359–3372.

Couillard-Despres, S., Winner, B., Schaubeck, S., Aigner, R., Vroemen, M., Weidner, N., et al., 2005. Doublecortin expression levels in adult brain reflect neurogenesis. Eur. J. Neurosci. 21, 1–14.

Danzer, S.C., 2012. Depression, stress, epilepsy and adult neurogenesis. Exp. Neurol. 233, 22–32.

Feil, R., Wagner, J., Metzger, D., Chambon, P., 1997. Regulation of Cre recombinase activity by mutated estrogen receptor ligand-binding domains. Biochem. Biophys. Res. Commun. 237, 752–757.
Feng, R., Rampon, C., Tang, Y.P., Shrom, D., Jin, J., Kyin, M., et al., 2001. Deficient neurogenesis in forebrain-specific presenilin-1 knockout mice is associated with reduced clearance of hippocampal memory traces. Neuron 32, 911–926.
Fournier, N.M., Andersen, D.R., Botterill, J.J., Sterner, E.Y., Lussier, A.L., Caruncho, H.J., et al., 2010. The effect of amygdala kindling on hippocampal neurogenesis coincides with decreased reelin and DISC1 expression in the adult dentate gyrus. Hippocampus 20, 659–671.
Goddard, G.V., McIntyre, D.C., Leech, C.K., 1969. A permanent change in brain function resulting from daily electrical stimulation. Exp. Neurol. 25, 295–330.
Hattiangady, B., Shetty, A.K., 2008. Implications of decreased hippocampal neurogenesis in chronic temporal lobe epilepsy. Epilepsia 49 (Suppl. 5), 26–41.
Hattiangady, B., Shetty, A.K., 2010. Decreased neuronal differentiation of newly generated cells underlies reduced hippocampal neurogenesis in chronic temporal lobe epilepsy. Hippocampus 20, 97–112.
Hattiangady, B., Rao, M.S., Shetty, A.K., 2004. Chronic temporal lobe epilepsy is associated with severely declined dentate neurogenesis in the adult hippocampus. Neurobiol. Dis. 17, 473–490.
Hawrylak, N., Chang, F.L., Greenough, W.T., 1993. Astrocytic and synaptic response to kindling in hippocampal subfield CA1. II. Synaptogenesis and astrocytic process increases to in vivo kindling. Brain Res. 603, 309–316.
Imayoshi, I., Sakamoto, M., Ohtsuka, T., Takao, K., Miyakawa, T., Yamaguchi, M., et al., 2008. Roles of continuous neurogenesis in the structural and functional integrity of the adult forebrain. Nat. Neurosci. 11, 1153–1161.
Jakubs, K., Nanobashvili, A., Bonde, S., Ekdahl, C.T., Kokaia, Z., Kokaia, M., et al., 2006. Environment matters: synaptic properties of neurons born in the epileptic adult brain develop to reduce excitability. Neuron 52, 1047–1059.
Jessberger, S., Nakashima, K., Clemenson Jr., G.D., Mejia, E., Mathews, E., Ure, K., et al., 2007. Epigenetic modulation of seizure-induced neurogenesis and cognitive decline. J. Neurosci. 27, 5967–5975.
Kawamoto, S., Niwa, H., Tashiro, F., Sano, S., Kondoh, G., Takeda, J., et al., 2000. A novel reporter mouse strain that expresses enhanced green fluorescent protein upon Cre-mediated recombination. FEBS Lett. 470, 263–268.
Kempermann, G., Wiskott, L., Gage, F.H., 2004. Functional significance of adult neurogenesis. Curr. Opin. Neurobiol. 14, 186–191.
Khurgel, M., Ivy, G.O., 1996. Astrocytes in kindling: relevance to epileptogenesis. Epilepsy Res. 26, 163–175.
Kokaia, M., 2011. Seizure-induced neurogenesis in the adult brain. Eur. J. Neurosci. 33, 1133–1138.
Lagace, D.C., Whitman, M.C., Noonan, M.A., Ables, J.L., DeCarolis, N.A., Arguello, A.A., et al., 2007. Dynamic contribution of nestin-expressing stem cells to adult neurogenesis. J. Neurosci. 27, 12623–12629.
Longo, B., Romariz, S., Blanco, M.M., Vasconcelos, J.F., Bahia, L., Soares, M.B., et al., 2010. Distribution and proliferation of bone marrow cells in the brain after pilocarpine-induced status epilepticus in mice. Epilepsia 51, 1628–1632.
Loscher, W., Brandt, C., 2010. Prevention or modification of epileptogenesis after brain insults: experimental approaches and translational research. Pharmacol. Rev. 62, 668–700.
Mandyam, C.D., Harburg, G.C., Eisch, A.J., 2007. Determination of key aspects of precursor cell proliferation, cell cycle length and kinetics in the adult mouse subgranular zone. Neuroscience 146, 108–122.
McIntyre, D.C., Poulter, M.O., Gilby, K., 2002. Kindling: some old and some new. Epilepsy Res. 50, 79–92.
Meltzer, L.A., Yabaluri, R., Deisseroth, K., 2005. A role for circuit homeostasis in adult neurogenesis. Trends Neurosci. 28, 653–660.
Mori, T., Tanaka, K., Buffo, A., Wurst, W., Kuhn, R., Gotz, M., 2006. Inducible gene deletion in astroglia and radial glia—a valuable tool for functional and lineage analysis. GLIA 54, 21–34.
Murphy, B.L., Pun, R.Y., Yin, H., Faulkner, C.R., Loepke, A.W., Danzer, S.C., 2011. Heterogeneous integration of adult-generated granule cells into the epileptic brain. J. Neurosci. 31, 105–117.
Nakamura, T., Colbert, M.C., Robbins, J., 2006. Neural crest cells retain multipotential characteristics in the developing valves and label the cardiac conduction system. Circ. Res. 98, 1547–1554.
Ninkovic, J., Mori, T., Gotz, M., 2007. Distinct modes of neuron addition in adult mouse neurogenesis. J. Neurosci. 27, 10906–10911.
Parent, J.M., Murphy, G.G., 2008. Mechanisms and functional significance of aberrant seizure-induced hippocampal neurogenesis. Epilepsia 49 (Suppl. 5), 19–25.
Parent, J.M., Janumpalli, S., McNamara, J.O., Lowenstein, D.H., 1998. Increased dentate granule cell neurogenesis following amygdala kindling in the adult rat. Neurosci. Lett. 247, 9–12.
Parent, J.M., Tada, E., Fike, J.R., Lowenstein, D.H., 1999. Inhibition of dentate granule cell neurogenesis with brain irradiation does not prevent seizure-induced mossy fiber synaptic reorganization in the rat. J. Neurosci. 19, 4508–4519.
Parent, J.M., Valentin, V.V., Lowenstein, D.H., 2002. Prolonged seizures increase proliferating neuroblasts in the adult rat subventricular zone-olfactory bulb pathway. J. Neurosci. 22, 3174–3188.
Pauli, E., Hildebrandt, M., Romstock, J., Stefan, H., Blumcke, I., 2006. Deficient memory acquisition in temporal lobe epilepsy is predicted by hippocampal granule cell loss. Neurology 67, 1383–1389.
Paxinos, G., Franklin, K.B.J., 2004. The mouse brain in sterotaxic coordinates, 2nd edition. Academic Press, Elsevier Science, San Diego USA.
Pekcec, A., Muhlenhoff, M., Gerardy-Schahn, R., Potschka, H., 2007. Impact of the PSA-NCAM system on pathophysiology in a chronic rodent model of temporal lobe epilepsy. Neurobiol. Dis. 27, 54–66.
Pekcec, A., Fuest, C., Muhlenhoff, M., Gerardy-Schahn, R., Potschka, H., 2008. Targeting epileptogenesis-associated induction of neurogenesis by enzymatic depolysialylation of NCAM counteracts spatial learning dysfunction but fails to impact epilepsy development. J. Neurochem. 105, 389–400.
Pekcec, A., Lupke, M., Baumann, R., Seifert, H., Potschka, H., 2011. Modulation of neurogenesis by targeted hippocampal irradiation fails to affect kindling progression. Hippocampus 21, 866–876.
Racine, R.J., 1972. Modification of seizure activity by electrical stimulation. II. Motor seizure. Electroencephalogr. Clin. Neurophysiol. 32, 281–294.
Rogawski, M.A., 2005. Astrocytes get in the act in epilepsy. Nat. Med. 11, 919–920.
Scharfman, H.E., McCloskey, D.P., 2009. Postnatal neurogenesis as a therapeutic target in temporal lobe epilepsy. Epilepsy Res. 85, 150–161.
Scharfman, H.E., Goodman, J.H., Sollas, A.L., 2000. Granule-like neurons at the hilar/CA3 border after status epilepticus and their synchrony with area CA3 pyramidal cells: functional implications of seizure-induced neurogenesis. J. Neurosci. 20, 6144–6158.
Scott, B.W., Wang, S., Burnham, W.M., De Boni, U., Wojtowicz, J.M., 1998. Kindling-induced neurogenesis in the dentate gyrus of the rat. Neurosci. Lett. 248, 73–76.
Seeger, N., Zellinger, C., Rode, A., Roloff, F., Bicker, G., Russmann, V., et al., 2011. The erythropoietin-derived peptide mimetic pHBSP affects cellular and cognitive consequences in a rat post-status epilepticus model. Epilepsia 52, 2333–2343.
Seifert, G., Carmignoto, G., Steinhauser, C., 2010. Astrocyte dysfunction in epilepsy. Brain Res. Rev. 63, 212–221.
Shapiro, L.A., Ribak, C.E., 2005. Integration of newly born dentate granule cells into adult brains: hypotheses based on normal and epileptic rodents. Brain Res. Brain Res. Rev. 48, 43–56.
Taupin, P., 2007a. BrdU immunohistochemistry for studying adult neurogenesis: paradigms, pitfalls, limitations, and validation. Brain Res. Rev. 53, 198–214.
Taupin, P., 2007b. Protocols for studying adult neurogenesis: insights and recent developments. Regen. Med. 2, 51–62.
Tian, G.F., Azmi, H., Takano, T., Xu, Q., Peng, W., Lin, J., et al., 2005. An astrocytic basis of epilepsy. Nat. Med. 11, 973–981.
Vezzani, A., Aronica, E., Mazarati, A., Pittman, Q.J., 2011. Epilepsy and brain inflammation. Exp. Neurol. (Electronic publication ahead of print).
Wiskott, L., Rasch, M.J., Kempermann, G., 2006. A functional hypothesis for adult hippocampal neurogenesis: avoidance of catastrophic interference in the dentate gyrus. Hippocampus 16, 329–343.
Wood, J.C., Jackson, J.S., Jakubs, K., Chapman, K.Z., Ekdahl, C.T., Kokaia, Z., et al., 2011. Functional integration of new hippocampal neurons following insults to the adult brain is determined by characteristics of pathological environment. Exp. Neurol. 229, 484–493.
Zhan, R.Z., Timofeeva, O., Nadler, J.V., 2010. High ratio of synaptic excitation to synaptic inhibition in hilar ectopic granule cells of pilocarpine-treated rats. J. Neurophysiol. 104, 3293–3304.